Breast Cancer Research and Treatment (2005) 89: 179–185

Report

Automatic ultrasound segmentation and morphology based diagnosis of solid breast tumors

Ruey-Feng Chang[1], Wen-Jie Wu[1], Woo Kyung Moon[2], and Dar-Ren Chen[3]
[1]*Department of Computer Science and Information Engineering, National Chung Cheng University, Chiayi, Taiwan;* [2]*Department of Diagnostic Radiology, Seoul National University Hospital, South Korea;* [3]*Department of Surgery, Changhua Christian Hospital, Changhua, Taiwan*

Key words: breast ultrasound, computer-aided diagnosis, level set, shape, support vector machine

Summary

Ultrasound (US) is a useful diagnostic tool to distinguish benign from malignant masses of the breast. It is a very convenient and safe diagnostic method. However, there is a considerable overlap benignancy and malignancy in ultrasonic images and interpretation is subjective. A high performance breast tumors computer-aided diagnosis (CAD) system can provide an accurate and reliable diagnostic second opinion for physicians to distinguish benign breast lesions from malignant ones. The potential of sonographic texture analysis to improve breast tumor classifications has been demonstrated. However, the texture analysis is system-dependent. The disadvantages of these systems which use texture analysis to classify tumors are they usually perform well only in one specific ultrasound system. While Morphological based US diagnosis of breast tumor will take the advantage of nearly independent to either the setting of US system and different US machines. In this study, the tumors are segmented using the newly developed level set method at first and then six morphologic features are used to distinguish the benign and malignant cases. The support vector machine (SVM) is used to classify the tumors. There are 210 ultrasonic images of pathologically proven benign breast tumors from 120 patients and carcinomas from 90 patients in the ultrasonic image database. The database contains only one image from each patient. The ultrasonic images are captured at the largest diameter of the tumor. The images are collected consecutively from August 1, 1999 to May 31, 2000; the patients' ages ranged from 18 to 64 years. Sonography is performed using an ATL HDI 3000 system with a L10-5 small part transducer. In the experiment, the accuracy of SVM with shape information for classifying malignancies is 90.95% (191/210), the sensitivity is 88.89% (80/90), the specificity is 92.5% (111/120), the positive predictive value is 89.89% (80/89), and the negative predictive value is 91.74% (111/121).

Introduction

Breast cancer has affected one of every eight women in United States and one of every ten women in Europe [1]. Early diagnoses of breast cancer are important. However, early diagnosis requires an accurate and reliable diagnostic procedure that allows physicians to distinguish benign breast tumors from malignant ones. Although there are many diagnostic modalities, biopsy is the best way to do the differential diagnosis. For the lawful and safe reasons, surgeons perform an even increasing number of breast biopsies. However, it is invasive and expensive. Biopsies are sometimes avoidable for the reason that probability of positive findings at biopsy for cancer is low, between 10% and 31% [2–4]. Ultrasound (US) is a useful diagnostic tool to distinguish benign from malignant masses of the breast [5]. However, there is a considerable overlap benignancy and malignancy in ultrasonic images and interpretation is subjective. Stavros et al. [6] reported the frequency with which certain morphological features were associated with breast cancer. Several of malignant features referred to the margin of the mass. Descriptors of mass margins associated with a high likelihood of malignancy include: (a) Angular margins in which obtuse or acute pointed junctions form between the mass and surrounding tissue; (b) Speculation in which alternating hypoechoic and hyperechoic lines radiate in multiple directions from the mass into the surrounding tissue; (c) Microlobulation characterized by greater than 3 lobulations of the mass surface.

Many techniques have been explored in the segmentation of medical images; however, segmentation of ultrasonic images is difficult due to the existence of noise and speckle. The conventional edge-based [7] and region-based methods [8,9] cannot work well in segmenting ultrasonic images. The newly developed level set approach is a kind of deformable model. This method was

begun by Osher and Sethian [10] in the Sethian's Ph.D. thesis. Comparing with other classical deformable model, such as snake [11], the principle of the level set approach is an active contour energy minimization that solves the computation of geodesics or minimal distance curves. It is governed by the curvature-dependent speeds of moving curves or fronts. At present, there have been many successful ultrasound segmentation researches using the level set approaches proposed [12–14].

Support vector machines (SVM) [15–17] have been recently proposed as a very effective method for pattern recognition, machine learning and data mining. It is considered a good candidate because of its high generalization performance. Intuitively, given a set of points which belongs to either one of two classes, a SVM can find a hyperplane leaving the largest possible fraction of points of the same class on the same side, while maximizing the distance of either class from the hyperplane. According to [15], this hyperplane, called optimal separating hyperplane (OSH), can minimize the risk of misclassifying examples of the test set. In this study we evaluated a set of breast US images using SVM and shape information for classifying breast tumors. Tumors are first segmented by the level set method and then six morphologic features are used.

Materials and methods

Image data acquisition and feature extraction

The US breast image databases include only histologically confirmed cases; 90 malignant tumors and 120 benign tumors which were recorded from August 1, 1999 to May 31, 2000. The ages of the patients were ranged from 18 to 64 years. All the digital images were obtained prior to biopsy using by an ATL HDI 3000 system with a L10-5 small part transducer which is a linear-array transducer with a frequency of 5–10 MHz and a scan width of 38 mm. All the images were supplied by one of the author (Dr. Moon). The region of interest (ROI) which contains the tumor was selected by one of the author (Dr. Chen). Through out this study, only the ROI sub-images are used to investigate the texture characteristics of benign and malignant lesions. Note that only one lesion is extracted from a patient.

The monochrome ultrasonic images are quantized into 8 bits, i.e. 256 gray levels and the features were stored via the magneto–optical (MO) disks. Then these images can be analyzed in a personal computer and serve as our experimental data. All solid nodules at US belong over C3 according to ACR (American College of Radiology) Breast Imaging Reporting and Data System (BI-RADS) category. We will utilize these images as our breast images database to further investigate the shape characteristics of benign and malignant tumors.

Morphologic feature extraction

Benign tumors usually have smooth shape and malignant tumors tend to have irregular border. According to this hypothesis, six morphologic features were extracted from each tumor to account for such sonographic features. These features are form_factor, roundness, aspect_ratio, convexity, solidity, and extent, respectively. Each feature is defined as follows:

$$1.\ \text{Form\_Factor} = \frac{4\pi \cdot \text{Area}}{\text{Perimeter}^2}, \tag{1}$$

$$2.\ \text{Roundness} = \frac{4 \cdot \text{Area}}{\pi \cdot \text{Max\_Diameter}^2}, \tag{2}$$

$$3.\ \text{Aspect\_Ratio} = \frac{\text{Max\_Diameter}}{\text{Min\_Diameter}} \tag{3}$$

$$4.\ \text{Convexity} = \frac{\text{Convex\_Perimeter}}{\text{Perimeter}}, \tag{4}$$

$$5.\ \text{Solidity} = \frac{\text{Convex\_Area} - \text{Area}}{\sum_{i=1}^{N} \text{Convex\_Area}_i - \text{Area}_i / N} \tag{5}$$

$$6.\ \text{Extent} = \frac{\text{Area}}{\text{Bounding\_Rectangle}}, \tag{6}$$

where Area and Perimeter is the area and perimeter of the tumor, Max_Diameter and Min_Diameter are the maximal and minimal dimensions of a tumor at different projection angles, as shown in Figure 1, Convex_Perimeter and Convex_Area are the perimeter and area of the convex hull of a tumor, N is the number of tumors in database, and Bounding_Rectangle is the area of the minimal rectangle including the tumor. We show the convex hull and bounding rectangle of a tumor in Figures 2 and 3, respectively.

By the way, when we find Max_Diameter, Min_Diameter, and Bounding_Rectangle, the US images should be rotated at different angles and then the maximal and minimal features can be found. Because of

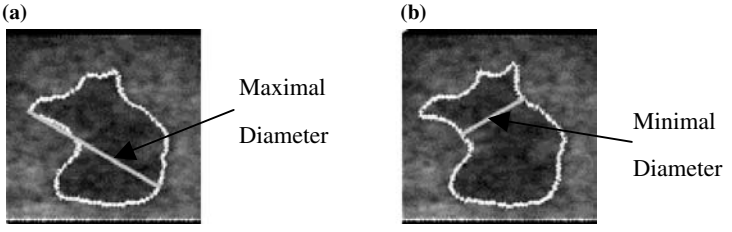

Figure 1. The maximal and minimal diameters of a tumor. (a) Maximal diameter (b) minimal diameter.

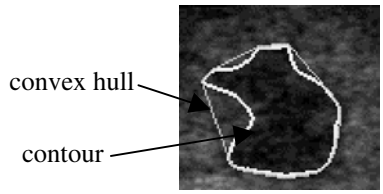

Figure 2. The convex hull and contour of a tumor.

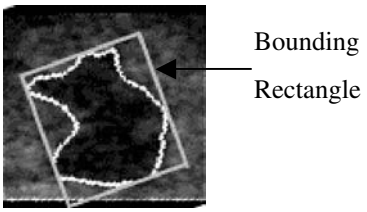

Figure 3. The bounding rectangle of a tumor.

the symmetry property and computation reduction, we only consider the rotation angles from 0° to 180° and the interval is 10°. We illustrate the rotated tumors at different angles in Figure 4.

Tumor segmentation

Due to the noise and speckles in the ultrasonic images, first, some noise filtering and edge-enhanced method are needed to reduce the noise and enhance the edge information in ultrasonic images. And then, the segmentation method will work more efficiently. In this section, the pre-processing and segmentation methods used in this paper are described.

Anisotropic diffusion filtering

There are several fundamental requirements of the noise filtering methods for medical images. First, it should not to lose the important information for object boundaries and detailed structures, second, it should efficiently remove the noise in the homogeneous regions, and third, it should enhance morphological definition by sharpening discontinuities [18].

The anisotropic diffusion filter [19] can get rid of the major drawback of the conventional spatial filters and improve the image quality significantly while preserve the important boundary information. The power of the anisotropic smoothing scheme lies in its dealing with local estimates of the image structures. Smoothing is formulated as a diffusive process, suppressed or stopped at boundaries by selecting locally adaptive diffusion strengths. Hence, in this filter, the smoothing operation could be prevented from across edges, the discontinuities can be preserved, and a weak slope remains nearly unchanged if the slope falls within the monotonically increasing part of the gradient values.

Stick method

In order to obtain a better segmentation result in ultrasonic images, conventional edge-detection algorithms usually use a low-pass filter to reduce the speckle noise, at the cost of blurring the edges. However, if the contrast of the edge is high, the influence of blurring can be reduced and not significantly impact the segmentation result [20]. Hence, the edge information should be enhanced for a better segmentation result.

In this study, the anisotropic diffusion filter is used to avoid the blurry problem of conventional low-pass filter and then the stick method is applied to further reduce noise and enhance the edge information. In the ultrasonic images, boundaries between tissue layers will appear as all sorts of lines; therefore, the edge detection problem can be modeled as a line process [21]. The stick [21], as a set of short line segments of variable orientation, is able to locally approximate the boundaries and to reduce speckles as well as improve the edge information in the ultrasound images.

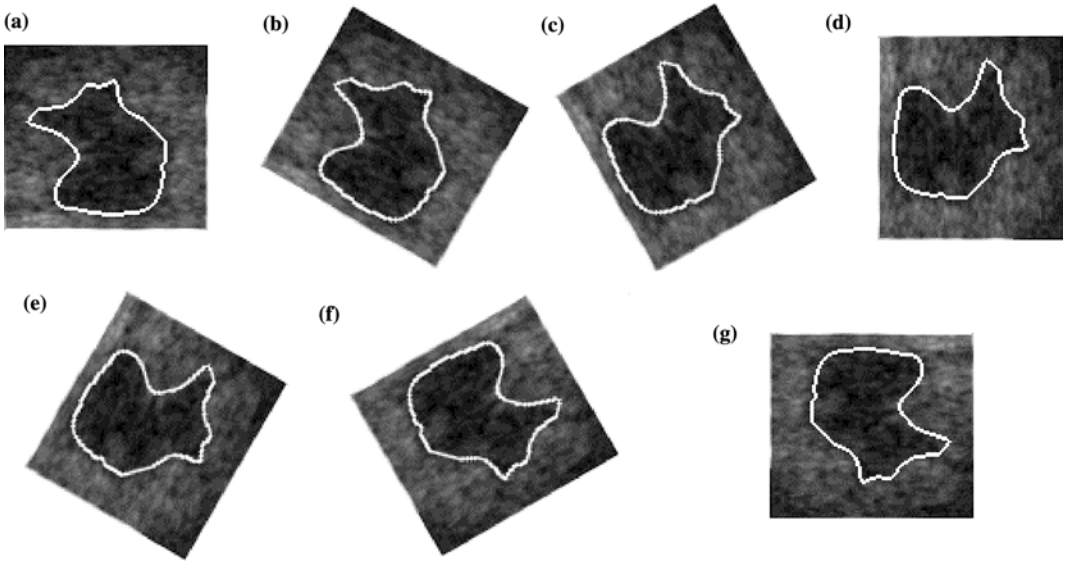

Figure 4. The rotated tumors at different angles. (a) 0° (b) 30° (c) 60° (d) 90° (e) 120° (f) 150° (g) 180°.

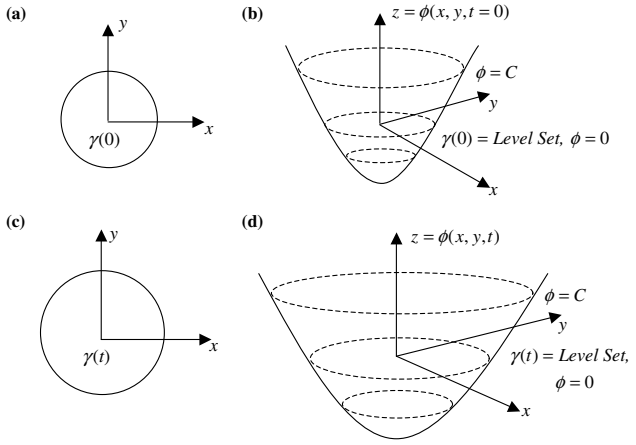

Figure 5. Level set curve propagation. (a) and (b) show the curve γ and the corresponding surface $\phi(x, y)$ at $t = 0$, and (c) and (d) show the curve γ and the corresponding surface $\phi(x, y)$ at time t.

Automatic thresholding method

In an ultrasonic image, the region of the tumor appears to be darker and the background is brighter. After the image processed through the anisotropic diffusion filter and stick method, we use the thresholding scheme to turn an ultrasound gray level image into a binary one to separate the tumor from its background. We adopt an automatic threshold-determination method, proposed by N. Otsu [22], which can choose the threshold to minimize the intraclass variance of the black and white pixels automatically. We also apply an additional control scheme to allow the user to change the threshold value when the user is not satisfied with the threshold value assigned by this automatic method.

Level set method

The level set method [10,23] is a numerical technique for computing and analyzing the front propagation. It offers a highly robust and accurate method for tracking interfaces moving under complex motions. Instead of propagating the front directly, it embeds the front as the zero level set of a higher order function called the level set function. (see Appendix 1)

In the proposed method, the original ultrasonic image is first processed by the anisotropic diffusion filtering, stick method, and thresholding method. After the thresholding method, we achieve a binary image and then combine it with the original image. When combining, the proportion of each image is 0.5. Finally, we utilize the level set method to segment the tumor in the combined image. A segmentation result is shown in Figure 6.

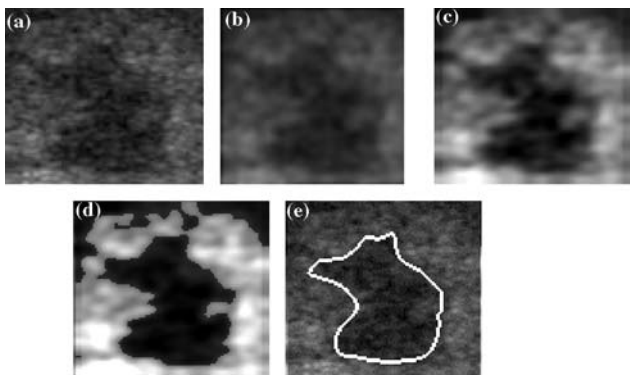

Figure 6. The tumor segmentation with the proposed method. (a) The original image (b) the image after the anisotropic diffusion filter (c) the image after the stick method (d) the image which combines the thresholded and original images (e) the result of level set method.

Classification with support vector machine model

SVM is a very good classification tool because of its high generalization performance. It has been proved as a very effective method for many applications. The concept of SVM and the general case of nonlinear separating surfaces were introduced in Appendix 2.

In this study, we use nonlinear SVM with Gaussian radial basis kernel as our classifier. The shape information is used as the inputs to find an OSH for distinguishing the benign tumors from malignant ones.

Result

In our experiments, we totally use 210 pathology-proven cases (including 120 benign breast tumors and 90 malignant ones) to test the classification accuracy of the proposed method. These ultrasonic images are randomly divided into five groups. We first set the first group as a testing group and use the remaining four groups to train the SVM. After training, the SVM is then tested on the first group. Then we set the second group as a testing group and the remaining four groups are trained and then the SVM is tested on the second. This process is repeated until all five groups have been set in turn as a testing group.

In this work, we first use some preprocessing and level set methods to segment the tumor of an ultrasonic image. And then we use a nonlinear SVM with Gaussian radial basis kernel as our classifier where C and γ are 3 and 0.074, respectively. Six morphologic features are used as the input of the SVM to classify the experimental cases. In Figure 8, we compare the six morphologic features between benign tumors and malignant ones. These simulations are made on a single CPU Intel Pentium-VI 2 GHz personal computer with Microsoft Windows XP operating system. We list the experimental result in Table 1 and show the ROC analysis in Figure 9.

To estimate the performance of the experimental result, five objective indices are used. These indices are accuracy, sensitivity, specificity, positive predictive value, and negative predictive value. In our experiment,

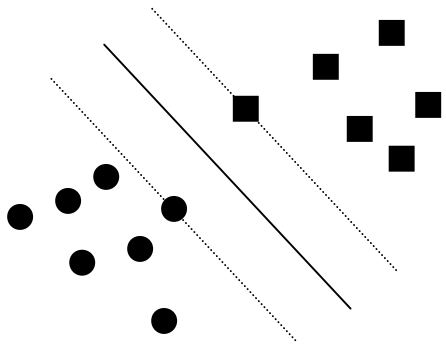

Figure 7. Separating hyperplane. (The dashed lines identify the margin.)

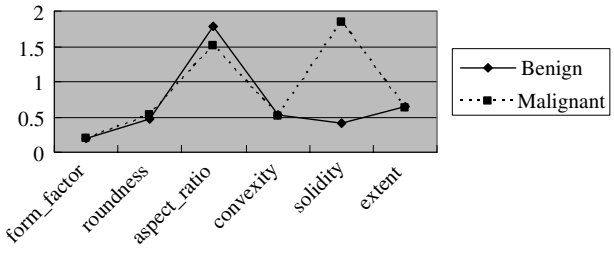

Figure 8. Comparison of six morphologic features between benign tumors and malignant ones.

Table 1. Classification of breast tumors by SVM with shape feature

Sonographic classification	Benign[a]	Malignant[a]
Benign	TN 111	FN 10
Malignant	FP 9	TP 80
Total	120	90

Note: TP, True Positive; TN, True Negative; FP, False Positive; FN, False Negative
[a] Histological finding.

Table 2. The objectively indices result for the proposed method

Index	Performance
Accuracy	90.95%
Sensitivity	88.89%
Specificity	92.50%
PPV	89.89%
NPV	91.74%

Note:
Accuracy = (TP + TN) / (TP + TN + FP + FN)
Sensitivity = TP / (TP + FN)
Specificity = TN / (TN + FP)
Positive Predictive Value = TP / (TP + FP)
Negative Predictive Value = TN / (TN + FN)

the accuracy of SVM with shape information for classifying malignancies is 90.95% (191/210), the sensitivity is 88.89% (80/90), the specificity is 92.5% (111/120), the positive predictive value is 89.89% (80/89), and the negative predictive value is 91.74% (111/121). We also list these indices in Table 2. According to the Table 2 and Figure 9, we can conclude that the classification ability for breast tumors with shape information is very well.

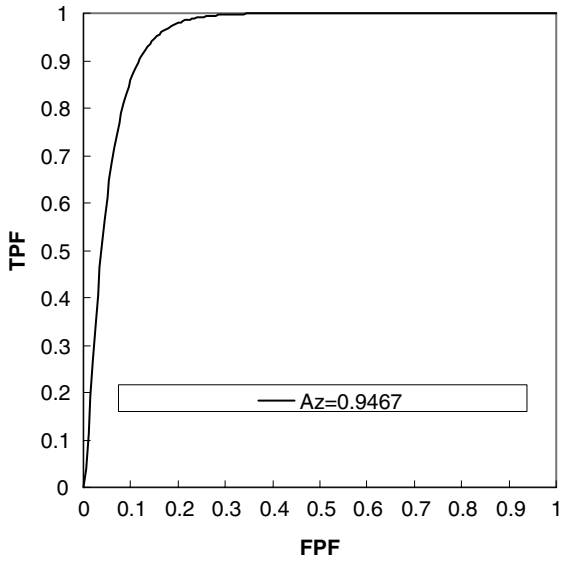

Figure 9. The ROC analysis of the proposed method.

Conclusion

Recent progress of computer-aided diagnosis (CADx) system demonstrated that the application of CADx system could increase the diagnostic confidence for a physician and provides one possible solution to improve the positive predictive value of breast biopsy. Although these proposed CAD system, examples from our previous works [24–26], could be readily adaptable to US machine; there is no available data to be verified whether a designed system was suitable to another US machine without any change or through the adjustment of the parameters by using intelligent selection algorithms according to the different US machines. In fact, with the rapid development of US technologies, many different ultrasonic systems are used in the current medical diagnosis. Subsequently, we successfully proposed adjustment schemes for different ultrasonic systems were used to transform needed information for the differential diagnosis [27]. However, this method still need collect different US machine data as well as machine setting parameters in advance. It could not be readily adaptable to new US machines. The aim of this study using automatic ultrasound segmentation and morphology based method is to improve this drawback; we believe that is valuable for future development of ultrasonic CAD system. The morphologic features describe the shape and contour of the lesion and the texture features characterize the image properties evolved from the intension distribution such as echogenicity and

echotexture. Texture features are helpful to classify benign and malignant tumors on sonography. The potential of sonographic texture analysis to improve breast tumor diagnosis has already been demonstrated [28–30]. However, the texture analysis is system-dependent. In other words, the disadvantages of these systems which use texture analysis to classify tumors are they usually perform well only in one specific ultrasound system. While Morphological based US diagnosis of breast tumor will take the advantage of nearly independent to either the setting of US system and different US machines. A CAD based on the shape analysis was proposed by Chen et al. [31] with good system performance. However, it relies on physicians to manually segment tumors. In this study, we further improved with an automatic tumor segmentation and shape analysis CAD system.

Appendix 1

Let $\gamma(0)$ be a closed initial planar curve in a Euclidean plane $\Re^2$, and let $\gamma(t)$ be the family of curves which is generated by the movement of the initial curve $\gamma(0)$ in the direction of its normal vector N. Moreover, we assume that the speed of this movement is a scalar function F of the curvature K.

The main idea in the level set approach is to represent the front $\gamma(t)$ as the level set [23] of a function ϕ. In other words, given a moving closed hypersurface $\gamma(t)$, that is, $\gamma(t=0)$: $[0,\infty) \rightarrow \Re^N$, we wish to produce a formulation for the motion of the hypersurface propagating along its normal direction with speed F. Hence, the idea of the level set methodology is to embed this propagating interface as the zero level set of a higher dimension function ϕ. The function ϕ is defined as follows. Let $\phi(x,t=0)$ for x is a point in $\Re^N$, be defined by

$$\phi(x, t=0) = \pm d, \tag{7}$$

where d is the distance from x to $\gamma(t=0)$, and the sign is chosen if the point x is outside (plus) or inside (minus) the initial hypersurface $\gamma(t=0)$. Thus, we have an initial function $\phi(x,t=0)$: $\Re^N \rightarrow \Re$ with the property that

$$\gamma(t=0) = (x|\phi(x, t=0) = 0). \tag{8}$$

The goal is to produce an equation for the evolving function $\phi(x,t)$, which contains the embedded motion of $\gamma(t)$ as the level set [23]. To do so, let $x(t)$ be the path of a point on the propagating front. That is $x(t=0)$ is a point on the initial front $\gamma(t=0)$, and $x_t \cdot n = F(x(t))$ with the vector x_t normal to the front at $x(t)$. Since the evolving function ϕ is always zero on the propagating hypersurface, we must have

$$\phi(x(t), t) = 0. \tag{9}$$

By the chain rule,

$$\phi_t + \nabla\phi(x(t), t) \cdot x'(t) = 0. \tag{10}$$

Since F supplies the speed in the outward normal direction, then $x'(t) \cdot n = F$ where $n = \nabla\phi/|\nabla\phi|$ and we have the evolution equation for ϕ, namely

$$\phi_t + F|\nabla\phi| = 0, \tag{11}$$

with a given value of $\phi(x,t=0)$. This is the level set equation introduced by Osher and Sethian [10].

To help illustrate these ideas, Figure 5 shows the outward propagation of an initial curve and the accompany motion of the level set function ϕ. Suppose the initial front γ at $t=0$ is a circle in the xy-plane, as shown in Figure 5(a). Thus, the circle is the level set [23] of an initial surface $z = \phi(x,y,t=0)$ in $\Re^3$, as shown in Figure 5(b). We can then match the moving curves $\gamma(t)$ in such a way that the level set [23] always yields the moving front, as shown in Figures 5(c) and (d).

Appendix 2

If there is a training example set $S, \{(x_i, y_i)_{1 \le i \le N}\}$, where $\mathbf{x}_i \in R^n$ and $y_i \in \{-1, 1\}$ is a class label. The goal of SVM is to define a hyperplane which divides S such that all the points with the same label are on the same side of the hyperplane while maximizing the distance between the two classes and the hyperplane, as shown in Figure 7. This means to find a pair ($\mathbf{w}$, b) such that

$$y_i(w \cdot x_i + b) > 1, \quad i = 1, \ldots, N \tag{12}$$

where $\mathbf{w} \in R^n$ and $b \in R$.

According to Equation (12), we can know the minimal distance between the closest point and the hyperplane is $1/\|\mathbf{w}\|$. Besides, the OSH is a hyperplane which the distance to the closest point is maximal. Hence, in order to find the OSH, we must minimize $\|\mathbf{w}\|^2$ under constraint Equation (12).

If we denote with $\boldsymbol{\alpha} = (\alpha_1, \alpha_2, \ldots, \alpha_N)$ the N nonnegative Lagrange multipliers associated with constraint Equation (12), the problem of finding OSH is Equivalent to the maximization of the function

$$W(\alpha) = \sum_{i=1}^{N} \alpha_i - \frac{1}{2} \sum_{i,j=1}^{N} \alpha_i \alpha_j y_i y_j \mathbf{x}_i \cdot \mathbf{x}_j, \tag{13}$$

where $\alpha_i \ge 0$ and under constraint $\sum_{i=1}^{N} y_i \alpha_i = 0$.

Once the vector $\bar{\boldsymbol{\alpha}} = (\bar{\alpha}_1, \bar{\alpha}_2, \ldots, \bar{\alpha}_N)$ solution of Equation (13) has been found, the OSH $(\bar{\mathbf{w}}, \bar{b})$ has the following expansion:

$$\bar{\mathbf{w}} = \sum_{i=1}^{N} \bar{\alpha}_i y_i x_i, \tag{14}$$

while $\bar{b}$ can be determined from $\bar{\boldsymbol{\alpha}}$ and from the Kühn–Tucker conditions [32]

$$\bar{\alpha}_i(y_i(\bar{\mathbf{w}} \cdot \mathbf{x}_i + \bar{b}) - 1) = 0, \quad i = 1, 2, \ldots, N. \tag{15}$$

By the way, the corresponding training examples $(\mathbf{x}_i, y_i)$ with nonzero coefficients α_i are called support vectors. At last, the decision function of classifying a new data point $\mathbf{x}$ can be written as:

$$f(\mathbf{x}) = \mathrm{sgn}(\sum_{i=1}^{N} \bar{\alpha}_i y_i \mathbf{x}_i \cdot \mathbf{x} + \bar{b}). \tag{16}$$

The training example set that we want to classify is usually linearly nonseparable. To achieve better generalization performance, the input data can first be mapped into a high-dimensional feature space. Then the OSH is constructed in the feature space.

If $\Phi(\mathbf{x})$ denotes a mapping function that maps $\mathbf{x}$ into a high-dimensional feature space, Equation (13) is then rewritten as follows:

$$W(\alpha) = \sum_{i=1}^{N} \alpha_i - \frac{1}{2} \sum_{i=1}^{N} \alpha_i \alpha_j y_i y_j \mathbf{\Phi}(\mathbf{x}_i) \mathrm{A} \mathbf{\Phi}(\mathbf{x}_\mathrm{j}). \tag{17}$$

Now, let $K(\mathbf{x}_i, \mathbf{x}_j) = \mathbf{\Phi}(\mathbf{x}_i) \cdot \mathbf{\Phi}(\mathbf{x}_j)$ we can rewrite Equation (17) as

$$W(\alpha) = \sum_{i=1}^{N} \alpha_i - \frac{1}{2} \sum_{i,j=1}^{N} \alpha_i \alpha_j y_i y_j K(\mathbf{x}_i, \mathbf{x}_j), \tag{18}$$

where K is called a kernel function and must satisfy Mercer's theorem [15]. Finally, the decision function becomes

$$f(\mathbf{x}) = \mathrm{sgn}(\sum_{i=1}^{N} \alpha_i y_i K(\mathbf{x}_i, \mathbf{x}) + b). \tag{19}$$

References

1. Pandey N, Salcic Z, Sivaswamy J: Fuzzy logic based microcalcification detection. neural networks for signal processing X, 2000. In: Proceedings of the 2000 IEEE Signal Processing Society Workshop 2000, Sydney, NSW, Australia, pp 662–671
2. Bassett LW, Liu TH, Giuliano AE, Gold RH: The prevalence of carcinoma in palpable vs impalpable, mammographically detected lesions. AJR 157: 21–24, 1991
3. Rubin M, Horiuchi K, Joy N, Haun W, Read R, Ratzer E, Fenoglio M: Use of fine needle aspiration for solid breast lesions is accurate and cost-effective. Am J Surg 174(6): 694–696, 1997
4. Gisvold JJ, Martin JK, Jr.: Prebiopsy localization of nonpalpable breast lesions. AJR Am J Roentgenol 143(3): 477–481, 1984
5. Shankar PM, Reid JM, Ortega H, Piccoli CW, Goldberg BB: Use of non-rayleigh statistics for identification of tumors in ultrasonic B-scans of the breast. IEEE Trans Med Imag 12: 687–692, 1993
6. Stavros AT, Thickman D, Rapp CL, Dennis MA, Parker SH, Sisney GA: Solid breast nodules: use of sonography to distinguish between benign and malignant lesions. Radiology 196(1): 123–134, 1995
7. Canny J: A computational approach to edge detection. IEEE Trans Pattern Anal Machine Intell 8(6): 679–698, 1986
8. Pavlidis T: Algorithms for Graphics and Image Processing. Computer Science Press, Rockville, MD, 1982
9. Pavlidis T, Horowitz SL: Segmentation of plane curves. IEEE Trans Comput 27(8): 860–870, 1974
10. Osher S, Sethian J: Fronts propagating with curvature-dependent speed: Algorithms based on Hamilton–Jacobi equations. J Comput Phys 79(1): 12–49, 1988
11. Kass M, Witkin A, Terzopoulos D: Snakes: active contour models. Int J Comp Vis 1(4): 321–331, 1988
12. Corsi C, Saracino G, Sarti A, Lamberti C: Left ventricular volume estimation for real-time three-dimensional echocardiography. IEEE Trans Med Imaging, 21(9): 1202–1208, 2002
13. Wang X, Wee WG: A new deformable contour method. In: Image Analysis and Processing, 1999. Proceeding International Conference on 1999, Venice, Italy, pp 430–435
14. Chen YM, Thiruvenkadam S, Tagare HD, Hung F, Wilson D, Geiser EA: On the incorporation of shape priors into geometric active contours. In: Variational and Level Set Methods in Computer Vision, 2001. Proceedings. IEEE Workshop on 2001, Vancouver, BC, Canada, pp 145–152
15. Vapnik VN: The Nature of Statistical Learning Theory. Springer-Verlag, New York, 1995
16. Chapelle O, Haffner P, Vapnik VN: Support vector machines for histogram-based image classification. IEEE Trans Neural Netw, IEEE Trans 10(5): 1055–1064, 1999
17. Pontil M, Verri A: Support vector machines for 3D object recognition. IEEE Trans Pattern Anal and Machine Intell 20(6): 637–646, 1998
18. Gerig G, Kubler O, Kikinis R, Jolesz FA: Nonlinear anisotropic filtering of MRI data. IEEE Trans Med Imaging 11(2): 221–232, 1992
19. Perona J, Malik J: Scale-scape and edge-detection using anisotropic diffusion. IEEE Trans Pattern Anal Machine Intell 12(7): 629–639, 1990
20. Czerwinski RN, Jones DL, O'Brien WD, Jr.: Edge detection in ultrasound speckle noise. Proc IEEE International Conference Image Processing, Austin, TX 1994, Austin, TX, pp 304–308
21. Czerwinski RN, Jones DL, O'Brien WD: Detection of lines and boundaries in speckle images - Application to medical ultrasound. IEEE Trans Med Imaging 18(2): 126–136, 1999
22. Otsu N: A threshold selection method form gray-level histograms. IEEE Trans Systems, Man, and Cybernetics 9(1): 62–66, 1979
23. Sethian JA: Level Set Methods: Evolving Interfaces in Geometry, Fluid Mechanics, Computer Vision, and Materials Science. Cambridge University Press, Cambridge, 1996
24. Chen DR, Chang RF, Huang YL, Chou YH, Tiu CM, Tsai PP: Texture analysis of breast tumors on sonograms. Semin Ultrasound CT MR 21(4): 308–316, 2000
25. Chen DR, Chang RF, Huang YL: Breast cancer diagnosis using self-organizing map for sonography. Ultrasound Med Biol 26(3): 405–411, 2000
26. Chen DR, Chang RF, Huang YL: Computer-aided diagnosis applied to US of solid breast nodules by using neural networks. Radiology 213(2): 407–412, 1999
27. Chen DR, Kuo WJ, Chang RF, Moon WK, Lee CC: Use of the bootstrap technique with small training sets for computer-aided diagnosis in breast ultrasound. Ultrasound Med Biol 28(7): 897–902, 2002
28. McPherson DD, Aylward PE, Knosp BM, Bean JA, Kerber RE, Collins SM, Skorton DJ: Ultrasound characterization of acute myocardial ischemia by quantitative texture analysis. Ultrason Imaging 8(4): 227–240, 1986
29. Garra BS, Krasner BH, Horii SC, Ascher S, Mun SK, Zeman RK: Improving the distinction between benign and malignant breast lesions: the value of sonographic texture analysis. Ultrason Imaging 15(4): 267–285, 1993
30. Goldberg V, Manduca A, Ewert DL, Gisvold JJ, Greenleaf JF: Improvement in specificity of ultrasonography for diagnosis of breast tumors by means of artificial intelligence. Med Phys 19(6): 1475–1481, 1992
31. Chen CM, Chou YH, Han KC, Hung GS, Tiu CM, Chiou HJ, Chiou SY: Breast lesions on sonograms: computer-aided diagnosis with nearly setting-independent features and artificial neural networks. Radiology 226(2): 504–514, 2003
32. Bertsekas DB, Tsitsiklis JN: Parallel and Distributed Computation: Numerical Methods. Prentice Hall, Englewood Cliffs, NJ, 1989

Address for offprints and correspondence: Dar-Ren Chen, Department of Surgery, Changhua Christian Hospital, 135 Nanhsiao Street, Changhua, Taiwan; *Tel.:* (886)-4-7238595; *Fax:* (886)-4-7228289; *E-mail:* dlchen88@ms13.hinet.net